FLOW PROFILE DEVELOPMENT IN THE UPSTREAM REGION FROM THE ENTRY PLANE OF A FLOW CONDUIT

SEK, JP; JANSSEN, LPBM

Published in:
Chemical Engineering Science

DOI:
10.1016/0009-2509(91)80065-7

Document Version
Publisher's PDF, also known as Version of record

Publication date:
1991

Chemical Engineering Science, Vol. 46, No. 10, pp. 2739–2748, 1991.
Printed in Great Britain.

0009–2509/91 $3.00 + 0.00

FLOW PROFILE DEVELOPMENT IN THE UPSTREAM REGION FROM THE ENTRY PLANE OF A FLOW CONDUIT

J. P. SEK[†] and L. P. B. M. JANSSEN[‡]
Department of Chemical Engineering, University of Groningen, Nijenborgh 16, 9747 AG Groningen, The Netherlands

(*Received* 14 *May* 1990; *accepted for publication* 8 *February* 1991)

Abstract—The development of flow profiles in the upstream region of a leading edge of a flat plate during laminar free surface flow has been studied. Results obtained experimentally by Laser Doppler Anemometry were in good agreement with numerical flow simulations using FLUENT program. An upstream distortion of the velocity profiles occurs in the whole range of Reynolds numbers investigated for laminar flow. From the distortions an approach length can be defined where the upstream influence of the stagnation point at the tip of the plate is noticeable. On the basis of the source theory an analytical model can be developed for the upstream changes of velocity. For viscous flows the source strength consists of a superposition of the classical expression for inviscous flow and a term proportional to the square root of the viscous length. It can be concluded that the hydrodynamic boundary layer for laminar flow has a finite thickness at the leading edge of the wall of a flow conduit.

1. INTRODUCTION

Flow in the inlet region of conduits of various cross-sections like rectangular channels, cylindrical tubes, concentric annuli etc. has been the subject of various publications over the past century. This hydrodynamic entry region for a steady laminar flow of incompressible Newtonian liquids has always been of interest for rheometrical measurements. Also the development of a theory for the onset of turbulence stimulated investigations in the inlet section of ducts. Nowadays, it is also recognized that the entry length is an important parameter for the design of heat exchangers or chemical reactors. Quite often for laminar flow of highly viscous liquids fully developed flow profiles are not obtained in this type of equipment.

Summaries of investigations on flow profile development in the inlet region of conduits can be found in several papers, for instance in review papers of van Dyke (1970) and Boger (1982). The approach most frequently used in the research on this subject was based on the boundary layer theory with the classical assumption of a *flat velocity profile* at the entrance of the flow conduit. Wang and Longwell (1964) were the first to realize that this assumption is rather arbitrary. They numerically solved the Navier–Stokes equations in full form for the case of flow in the inlet section of parallel plates. The calculations were performed for a Reynolds number of 300 and they showed that the development of the velocity flow profile can occur upstream from the entry plane of the flow conduit.

Similar numerical calculations of Vrentas *et al.* (1966) and Christiansen *et al.* (1972) for stream tube–real tube transition without contraction have shown upstream phenomena disappearing at values of Reynolds number above 250. However, the results of these numerical simulations are contrary to the findings reported by Astarita and Greco (1968) and Sylvester and Rosen (1970). By measuring the pressure drop in the entrance region of a cylindrical tube they concluded that a non-flat entry flow profile should exist and they deduced a possibility of upstream phenomena in the whole range of laminar flow, i.e. for Reynolds numbers up to 2000.

Presently, it is believed that above a certain value of Reynolds numbers—for instance 600 as assumed by Gupta and Garg (1981) or sufficiently high—[see Boger (1982); Mohanty and Asthana (1979); Tachibana (1981); Mohanty and Das (1982); Zirilli and Wirtz (1983); Gupta (1984); Soh (1987)] any upstream deviations are not significant. However, these assumptions are not confirmed by any detailed investigations concerning the velocity profile development in the upstream region. Also comprehensive experimental data pertaining to this problem are not available in the literature.

Therefore, the question still remains as to what is the precise shape of the velocity profiles in the liquid approaching an entry plane of a flow conduit. The solution of this problem would provide more comprehensive knowledge indispensable for the proper modelling of phenomena occurring in the inlet sections of flow systems.

2. PHYSICAL MODEL

The physical situation considered is that for an isothermal flow of viscous Newtonian liquid in a flow domain of infinite width in the z-direction (Fig. 1). In rectangular coordinates, the y–z plane at $x = 0$ represents the entry plane of the flow conduit. A wall of this conduit extends in the positive x-direction at $y = 0$. It is assumed that no slip occurs at its surface. The wall of the flow domain at $y = 0$ and for negative x is frictionless and can be regarded as a stream line.

[†]On leave from Institute of Chemical Engineering, Lodz Technical University, Lodz, Poland.
[‡]Author to whom correspondence should be addressed.

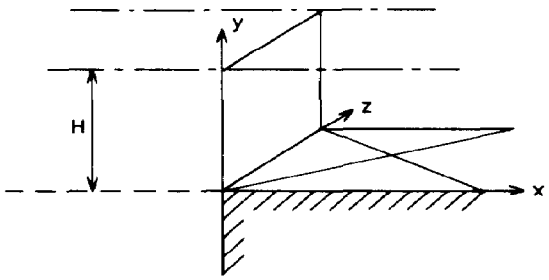

Fig. 1. Geometry of the flow domain.

The flow domain is bounded at the top at $y = H$. It is possible to define this upper boundary as a free surface. The case will then correspond to the situation at the entrance of an open horizontal channel in which steady-state laminar flow would occur. When the upper boundary is considered to be a symmetry plane the case is similar to that at the entrance between parallel plates, or after coordinate transformation to the flow in a stream tube–real tube transition without contraction.

Considering further the steady-state situation, let us assume that far upstream from the entry plane the flow profile is flat with only a velocity component in horizontal direction as shown in Fig. 2(a). Fluid elements transported in the plane of the surface of the wall ($y = 0$) will have to decelerate to meet the boundary conditions existing in the positive x-direction. The velocity of these fluid packets will decrease to zero at the leading edge of the wall where a stagnation point exists. It can be expected that existence of such a stagnation point will have an influence on the flow profile development in front of the entry plane of the flow system.

It is of course obvious that at the stagnation point as a result of transformation of kinetic to potential energy an excess develops as compared to the surrounding. This pressure rise for flows at high ratios of inertial to viscous forces will be close to that predicted directly from Bernoulli's equation as described for instance by Schlichting (1979). For flows at low values of this ratio the stagnation pressure will also be affected by viscous forces.

Because of pressure gradients in a horizontal direction the flat velocity profile will be deformed before it reaches the entry plane of the flow conduit [Fig. 2(a)]. Hence it is possible to predict that in the upstream region there will exist a distance termed "approach length" or "upstream length" where the flow profile is already developing. In principle the approach length and distortion of the flow profile will always occur, independent of the character of the flow as long as a stagnation point is present.

Of course, the pressure difference is not only restricted to the horizontal direction, but also exists between points along the y-axis. This pressure gradient will be responsible for a development of the flow in vertical direction [Fig. 2(b)].

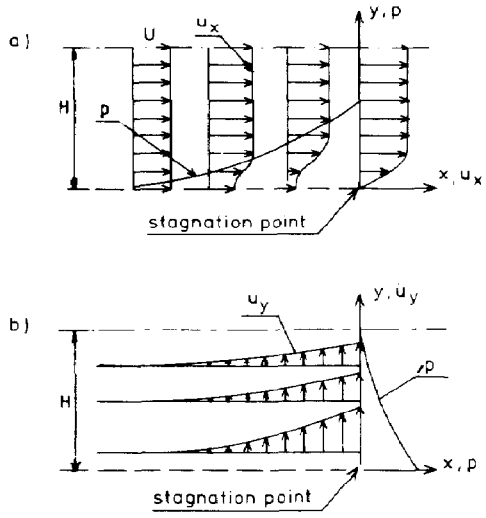

Fig. 2. Velocity profiles and pressure distribution in the upstream region of the stagnation point.

The detailed analyses of the flow in the upstream region is possible only on the basis of solving the equations of motion in full form [Wang and Longwell (1964)]. However, it seems possible that an analytical model can be proposed for the prediction of velocity changes in the x–z plane in negative x-direction.

Let us adopt for this purpose the concept of a source existing in a uniform stream of flowing liquid, e.g. Granger (1985). It is assumed that such a source of a strength q is placed on the surface of the wall of the flow conduit close to its leading edge as shown in Fig. 3. Velocity changes in the negative x-direction can be described by the following equation

$$u_x = U + \frac{q}{2\pi}\frac{1}{x - a_u} \tag{1}$$

where u_x is the local velocity along the x-axis, U is the velocity of the undisturbed flow far upstream and a_u is the distance between the leading edge of the wall and the centre of the source. A stagnation point at the leading edge of the wall can be obtained by defining the strength q of the source by

$$q = 2\pi U a_u \tag{2}$$

leading to

$$\frac{u_x}{U} = \frac{x}{x - a_u}. \tag{3}$$

This model predicts a zero velocity for $x = 0$ and an undisturbed velocity U for x approaching minus infinity. The degree of changes of the velocity along x-axis in the upstream region will be dependent on the strength of the source or on the distance a_u. The values of a_u and therefore, the source strength can be determined as a function of flow parameters on the basis of experiments and numerical simulations.

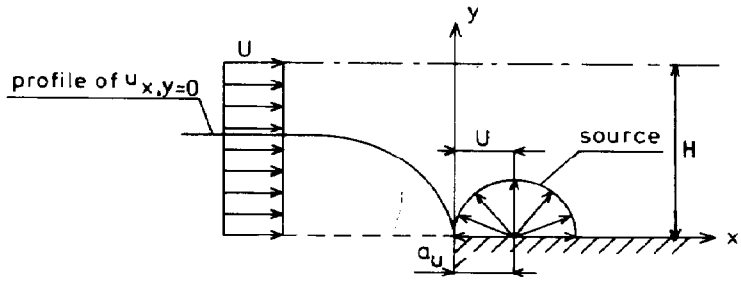

Fig. 3. Position of the source in the flow domain.

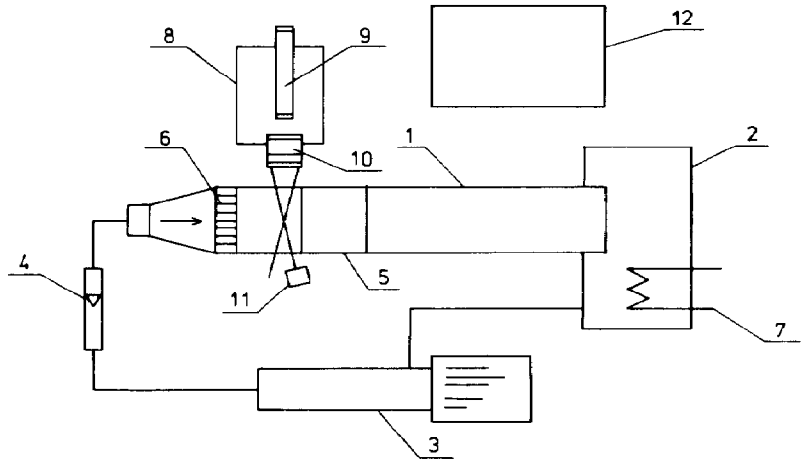

Fig. 4. Experimental equipment: (1) flow tunnel, (2) liquid storage tank, (3) Mohno pump, (4) rotameter, (5) flat plate, (6) flow distributor, (7) cooling system, (8) coordinate table, (9) laser, (10) beam splitting unit, (11) photodiode, and (12) signal processing units.

3. EXPERIMENTAL

The experiments consisted of Laser Doppler Anemometry in front of a flat plate parallel to the flow in a configuration as given in Fig. 4. The flow loop consisted of a liquid storage tank, a Mohno pump. rotameter and a flow tunnel. Copper coils and a thermobath were used to maintain a constant temperature of the circulating liquid. The flow tunnel consisted of a rectangular perspex box with a slowly diverging entrance section. The length of the tunnel was one meter and its cross-section 15 × 15 cm^2.

Close to half of the height of the tunnel a flat plate was placed horizontally. A knife-sharp edge of the plate prevented the occurrence of secondary flows in front of it. Most of the experiments were performed with a plate of 1 mm thickness. Control measurements were also carried out with a plate with a thickness of 0.2 mm. Despite of fivefold change in thickness no significant differences in flow profiles could be detected between the experiments, provided that the leading edges of the plates were very sharp.

An important constraint for the accuracy of the results was the existence of an undisturbed flat flow profile in the measurement region in absence of the plate. Therefore, the channel was not completely filled in order to allow for a free surface at the top of the fluid. Moreover, by adjusting the location of the plate, measurements could be performed in a domain where the influence of the side walls and the bottom was negligible. In order to ensure an appropriate velocity profile in the relevant section of the flow channel a flow distributor was placed at the end of the entrance section.

It was found during preliminary work that the most effective construction for the flow distributor was a combination of sheets of honeycomb material with layers of stainless steel gauze between them. The mesh of these metal gauzes was changed in the range 30–100 depending on flow rate and viscosity of the experimental fluid. The purpose of the metal gauze appeared to be twofold: because it prevented the fluid from fingering through sections of the honeycomb, it ensured a more flat flow profile and it eliminated pressure fluctuations originating from the pump. For the measurements aqueous solutions of glycerin with Newtonian behaviour were used as experimental media.

The flow in the tunnel was characterized by the

Reynolds number:

$$Re = \frac{H}{L_v} \tag{4}$$

where L_v is a viscous length defined as

$$L_v = \frac{\mu}{\rho U}. \tag{5}$$

U is an average velocity, H a characteristic height and μ and ρ are viscosity and density of the liquid, respectively.

For flow in the empty tunnel the Reynolds number based on the full height H_t of the liquid changed from 28.9 to 1190. The value 28.9 of the Reynolds parameter was the lowest one at which flat and almost undisturbed velocity profiles could be found in the upper part of the channel. In Fig. 5 two such profiles are presented. They were obtained experimentally for a distance l of about 0.2 and 0.3 m from the distributor and calculated for an average velocity U of the profile at 0.2 m. As seen from this graph, at a distance of about 0.1 m, differences in velocities did not exceeded 3% and decreased to zero in the plane where the plate was placed. It is known—see e.g. Boger (1982)—that during development of flow there is such a distance from the wall where the horizontal velocity remains almost constant.

Experimental verification also proved that the influence of side walls of the tunnel on the flow in the region of interest was negligible. It is obvious that at higher values of Re number the above problems were less significant.

The value of Re equal 1190 corresponds to the value 1820 if the hydraulic diameter of the flow in the channel is considered as a characteristic dimension. Above this value the increasing amplitude of oscillations did not allow us to obtain reliable data.

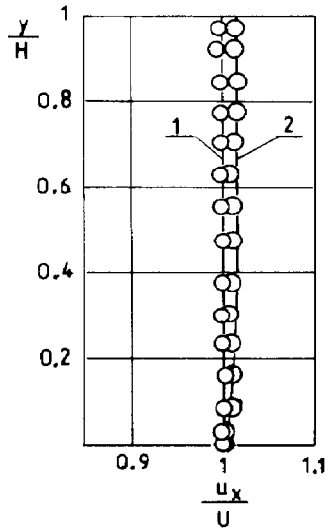

Fig. 5. Velocity profile development in the empty tunnel at $Re = 28.9$, (1) – $l = 0.2$ m, (2) – $l = 0.3$ m.

For the case of flow in the tunnel with the plate the parameter H was equal to the height of the liquid flowing over it and velocity U was equal to the undisturbed velocity in the upper part of the flow profiles. So defined, Re numbers changed in the range from 15.3 to 635 with corresponding changes of the viscous length from 0.00451 to 0.000109 m.

During the measurements, the Froude number based on the height of liquid in the tunnel H_t and defined as

$$Fr = \frac{U}{\sqrt{gH_t}} \tag{6}$$

varied in the range 0.0058–0.0239. At such small values of the Froude number no influence of the free surface should be noticed. Visual observations confirmed this.

The local horizontal velocities were measured using Laser Doppler Anemometry (LDA). Principles of this measuring technique have been published in many papers. The most comprehensive description can be found in Durst *et al.* (1976).

The LDA reference beam system used was developed by TNO (The Netherlands) and is presented schematically also in Fig. 4. It consisted of a 5 mW helium–neon laser and a beam splitting unit with rotating diffraction grating. After passing the flowing liquid the measuring beam was received by a photo diode. The output from this device was mixed with a reference beam signal coming from the beam splitting unit resulting in Doppler signals. After additional filtering Doppler frequencies were analysed using a digital oscilloscope–transiscope of Difa (Benelux). The transiscope allowed the direct determination of the average frequency of the signals. Additional fast Fourier transforms (FFT) provided detailed information about the basic frequency of the signals, their quality and a level of noise in the flow system.

The average and basic frequencies measured were transmitted from the transiscope to a computer where statistical processing of data was performed. Standard error calculations and the result of a t-test provided information on the number of samples to be taken in a single point to ensure statistical errors below 2%. The number of experiments per data point varied between 10 and 20, depending on the conditions of the flow in the system.

4. NUMERICAL SIMULATION

Numerical simulations of the flow were performed using the software package FLUENT version 2.99 provided by Flow Simulation Ltd (UK) and installed on a VAX-8650 computer. Calculations were carried out in Cartesian coordinates for a two-dimensional flow field.

Basic numerical calculations were performed for exactly the same flow conditions as those obtaining during experimental measurements. The length of the simulated flow domain was equal to the length of the plate plus a distance upstream superior to that where

experimentally deviations from a flat velocity profiles could be detected. The height of the cell was equal to the thickness of the liquid layer above the flat plate in the flow tunnel.

The bottom of the simulated flow domain along the length of the plate was defined using wall cells with a non-slip option. The part of the bottom corresponding to the free stream flow in front of the plate was represented by wall cells with a "link cut" in horizontal direction. This link-cut option allows us to perform calculations which simulate frictionless flow. Also the upper free surface of the flow domain was defined using the link-cut option.

The entry plane to the simulated flow domain was defined using input cells with boundary conditions that corresponded to a flat flow profile in this plane. The value of the entrance velocity was equal to the average velocity of flow in the corresponding plane on the basis of the LDA measurements. Also the physical parameters of the fluid were the same as those for the experimental media.

Numerical simulations were also performed for the same viscous lengths L_v of the flowing fluid as during experiments but with a height H of the flow domain increased fivefold and tenfold in relation to the experimental height. During this calculations the laminar character of the flow was imposed. Also the influence of the length of the wall was studied. Numerical cases with a plate ten times shorter and five times longer than the standard plate were also simulated.

During the calculations the steady-state momentum balance and the continuity equation in two-dimensional full form were solved:

$$-\rho(\nabla\cdot\mathbf{uu}) - [\nabla\cdot(p\boldsymbol{\delta} + \boldsymbol{\tau})] + \rho g = 0 \qquad (7)$$

$$\nabla\cdot\mathbf{u} = 0. \qquad (8)$$

The numerical simulations were performed in a grid with 80 nodes in horizontal and 60 nodes in vertical direction. The density of the vertical grid lines was the highest in the neighbourhood of the entry plane. The density of the horizontal grid lines increased towards the plate surface (see Fig. 6). During preliminary calculations the proper grid expansion in horizontal and vertical direction was established.

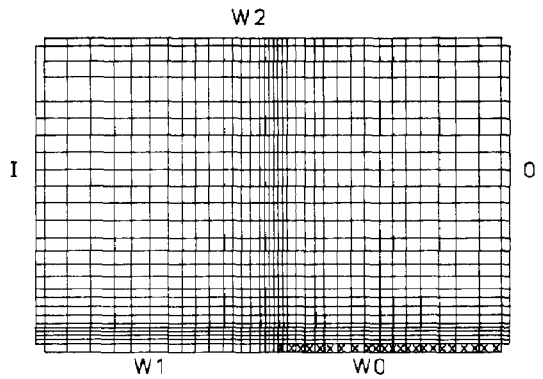

Fig. 6. Geometry and grid spacing of the computer simulated flow domain. I: input cells, O: output cells, WO: wall cells, W1, W2: wall cells with "cut link".

Depending on the case the expansion factor varied between 0.9 and 0.95 for contracting grids and between 1.05 and 1.1 for expanding grids. The number of nodes and the grid spacing were varied experimentally until grid-independent results were achieved. The underrelaxation factors were chosen experimentally in the range 0.2–0.6 for velocities and in the range 0.5–0.8 for pressure. The number of sweeps was also set by experience up to 2 for velocities and up to 8 for pressure.

During simulations the two discretization schemes "Power Law" and "QUICK" were used as described in *Fluent Manual* (1987). However, no distinct differences in the progress of the calculations and in the final results were observed.

All calculations proceeded until the sum of residuals was below 10^{-5}. It was found during preliminary calculations for known cases like flow in an open channel or between parallel plates that such an accuracy was necessary to achieve results converging to the analytical solutions.

The number of necessary iterations varied from about 2000 up to about 9000. The slowest convergence of the calculations was encountered for flows characterized by larger values of viscous length.

5. RESULTS AND DISCUSSION

Experimental measurements and numerical calculations were performed along the entire length of the flow domain considered. However, in this paper only phenomena occurring in the upstream region will be discussed.

The horizontal velocity profiles as obtained by experiments and numerical calculations are compared in Figs 7 and 8 both for the lowest and the highest Reynolds numbers used. Also for all other Reynolds numbers a good agreement between numerical and experimental data was obtained.

It is clearly evident from these figures that a development of the velocity profile already occurs in a region far upstream of the leading edge of the plate. The flow profiles in the entry plane of the plate (so at $x = 0$) are presented in Fig. 9 for the values of Reynolds numbers for which experiments were performed. They are supplemented by the results of a numerical simulation at a Reynolds number of 35,000 or $L_v = 1.94 \times 10^{-6}$ with a hypothetical preservation of the non-turbulent character of the flow. Also in this case distortion of the entry flow profile because of the stagnation point can be observed. These graphs show clearly that the boundary layer will have a finite thickness at the entry plane of the flow conduit. The direct consequence of this is also that the classical assumption of a flat velocity profile in front of the entry plane cannot be valid, at least for laminar flow.

The changes of the horizontal velocity in the upstream region along the plane which coincides with the upper surface of the plate ($y = 0$) are shown in

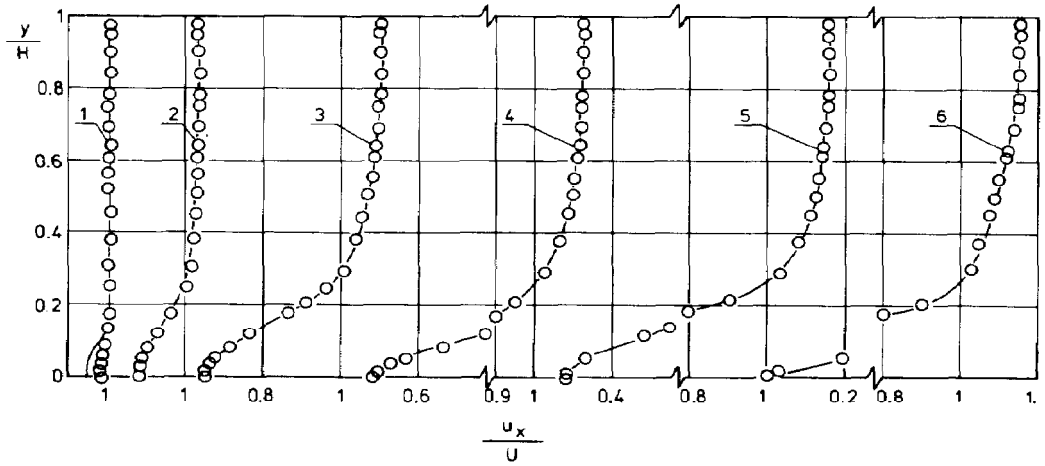

Fig. 7. Flow profile development in the upstream region for $Re = 15.3$ ($L_v = 4.51 \times 10^{-3}$ m): (1) $x = -0.1$ m, (2) $x = -0.02$ m, (3) $x = -0.01$ m, (4) $x = -0.005$ m, (5) $x = -0.002$ m, (6) $x = 0.0$ m. Experimental data points, numerical simulation.

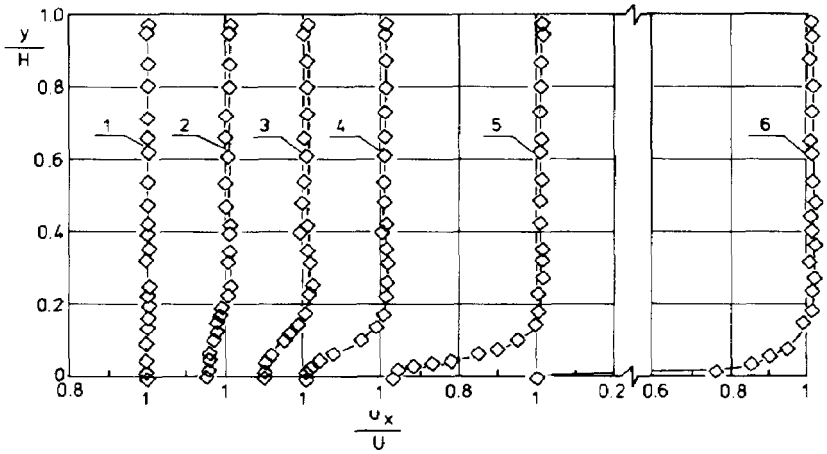

Fig. 8. Flow profile development in the upstream region for $Re = 635$ ($L_v = 1.09 \times 10^{-3}$ m): (1) $x = -0.08$ m, (2) $x = -0.02$ m, (3) $x = -0.01$ m, (4) $x = -0.005$ m, (5) $x = -0.002$ m, (6) $x = 0.0$ m. Experimental data points, numerical simulation.

Fig. 10 for values of the Re number and corresponding values of the viscous length for which investigations were performed. Here also the satisfactory agreement between numerical and experimental results can be noticed. From the graph in Fig. 10 it is also clear that the upstream influence of the stagnation point decreases with a decrease of the viscous length.

Two profiles from Fig. 10 obtained for $L_v = 0.00451$ m and $L_v = 0.000109$ m are compared in Fig. 11 with profiles calculated for the same values of L_v but at different heights H of the flow domain. Neglecting small differences resulting from coarser grid spacing it can be noticed that the height of the flow domain has no influence on phenomena occurring in the plane of the stagnation point ($y = 0$).

The same two profiles from Fig. 10 are compared in Fig. 12 with graphs calculated for different lengths of the plate. In this case also the influence of geometrical dimension on the deceleration of the flowing fluid can be neglected.

On the basis of these graphs one can conclude that in the geometry considered the upstream phenomena in the $y = 0$ plane are only dependent on the viscous length and independent of the physical dimensions. This result is confirmed by the well-known fact that the flat plate has no characteristic dimension.

For a quantitative characterization of the phenomena observed the model given by eq. (3) was used. To evaluate the parameter a_u the data points are redrawn in a coordinate system of $|x|/(u/U)$ versus upstream distance x as shown in Fig. 13. All sets of

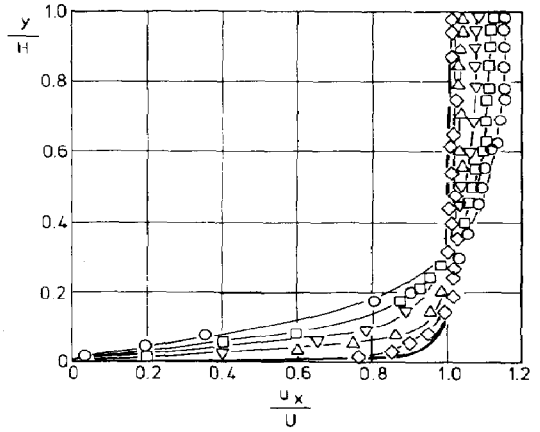

Fig. 9. Velocity profiles at the leading edge of the plate ($x = 0.0$ m). Experimental data points and numerical results. ○: $Re = 15.3$ ($L_v = 4.51 \times 10^{-3}$ m), □: $Re = 43.2$ ($L_v = 1.71 \times 10^{-3}$ m), ▽: $Re = 154$ ($L_v = 4.44 \times 10^{-3}$ m), △: $Re = 408$ ($L_v = 1.66 \times 10^{-3}$ m), ◇: $Re = 635$ ($L_v = 1.09 \times 10^{-3}$ m). Numerical results (——) $Re = 35{,}000$ ($L_v = 1.94 \times 10^{-6}$ m).

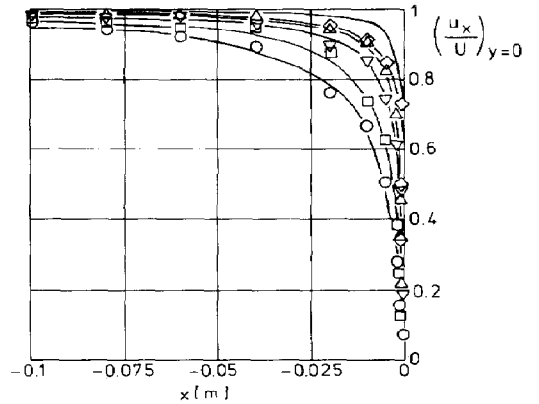

Fig. 10. Changes of the horizontal velocity in the $y = 0$ plane. Experimental data points and numerical results. ○: $Re = 15.3$ ($L_v = 4.51 \times 10^{-3}$ m), □: $Re = 43.2$ ($L_v = 1.71 \times 10^{-3}$ m), ▽: $Re = 154$ ($L_v = 4.44 \times 10^{-3}$ m), △: $Re = 408$ ($L_v = 1.66 \times 10^{-3}$ m), ◇: $Re = 635$ ($L_v = 1.09 \times 10^{-3}$ m). Numerical results (——) $Re = 35{,}000$ ($L_v = 1.94 \times 10^{-6}$ m).

points obtained for different values of Re could be approximated by straight lines. The absolute value of the slope of these lines varies in a small range between 0.985 and unity. For further considerations it is assumed that this slope equals unity for all sets of data. The accuracy of such an approach can be fully accepted from an engineering point of view. The ordinates of these straight lines at $x = 0$ are the values of the parameter a_u in eq. (3).

In Fig. 14 the relation between the values of a_u and $\sqrt{L_v}$ is presented. As it can be inferred from this graph the correlation between these two quantities could be approximated by a straight line given by

$$a_u = A + B\sqrt{L_v} \tag{9}$$

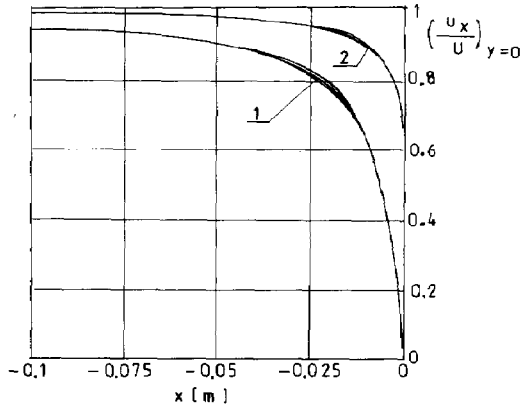

Fig. 11. The influence of the height of the flow domain on the velocity profile development in the $y = 0$ plane (explanations in the text). (1) $Re = 15.3$ ($L_v = 4.51 \times 10^{-3}$ m), (2) $Re = 635$ ($L_v = 1.09 \times 10^{-3}$ m).

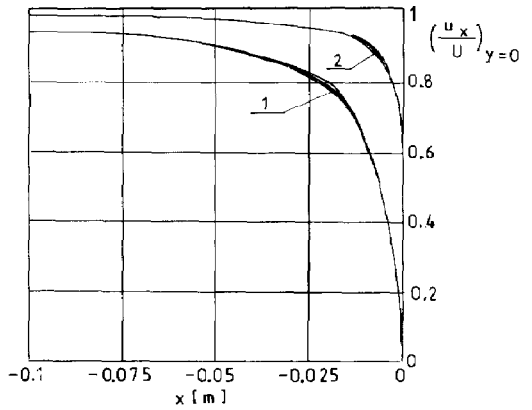

Fig. 12. The influence of the length of the plate on the velocity profile development in the $y = 0$ plane (explanations in the text). (1) $Re = 15.3$ ($L_v = 4.51 \times 10^{-3}$ m), (2) $Re = 635$ ($L_v = 1.09 \times 10^{-3}$ m).

where A and B are constants equal to, respectively, 0.000263 m and $0.0746\sqrt{\text{m}}$.

Equation (9) reveals that if the value of the viscous length approaches 0 with a non-zero viscosity and at non-slip condition parameter a_u becomes constant. It means that there will always be a source with a non-zero strength and, even when the ratio of inertial to viscous forces in the upstream region is very high, a distortion of velocity profiles can be expected. For creeping flows, at large values of the viscous length the influence of the stagnation point extends to large distances in front of the edge of the plate.

It has already been proved that geometric dimensions of the flow domain cannot be used for characterization of upstream phenomena in the $y = 0$ plane. However, it is still possible to make eq. (9) dimensionless using the asymptote of the source distance for the viscous length decreasing to zero as a character-

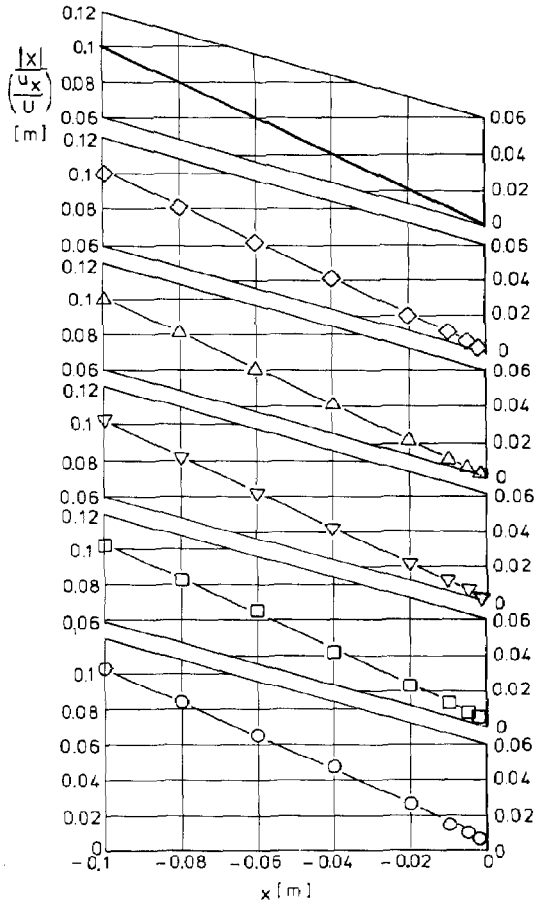

Fig. 13 The dependence of $|x|/(u_x/U)$ parameter on upstream distance x. Experimental data points and numerical results. ○: $Re = 15.3$ ($L_v = 4.51 \times 10^{-3}$ m), □: $Re = 43.2$ ($L_v = 1.71 \times 10^{-3}$ m), ▽: $Re = 154$ ($L_v = 4.44 \times 10^{-3}$ m), △: $Re = 408$ ($L_v = 1.66 \times 10^{-3}$ m), ◇: $Re = 635$ ($L_v = 1.09 \times 10^{-3}$ m). Numerical results (———) $Re = 35{,}000$ ($L_v = 1.94 \times 10^{-6}$ m).

istic length. Defining

$$Re_A = \frac{AU\rho}{\eta} \tag{10}$$

eq. (9) can be rewritten as

$$\frac{a_u}{A} = 1 + \frac{4.60}{\sqrt{Re_A}}. \tag{11}$$

Substitution of eq. (11) into eq. (3) gives a prediction of the changes of velocity in the upstream direction of the stagnation point.

$$\frac{u_x}{U} = \frac{x\sqrt{Re_A}}{\sqrt{Re_A}(x - 0.000263) - 0.00121}. \tag{12}$$

Figure 15 shows a comparison of the values of the dimensionless velocity u_x/U as predicted by eq. (12) with the values as obtained numerically with experimental confirmation and numerical data for $Re = 35{,}000$ ($L_v = 1.94 \times 10^{-6}$ m). The maximum error is within 5%.

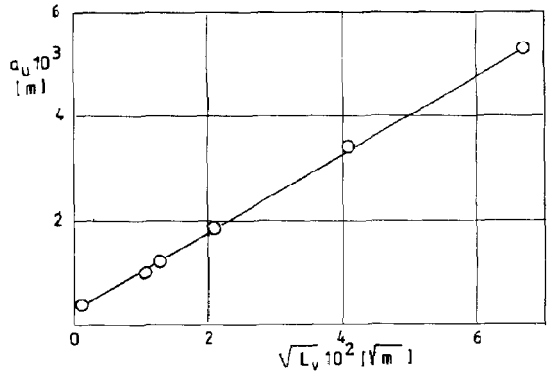

Fig. 14. The dependence of a_u parameter on the viscous length.

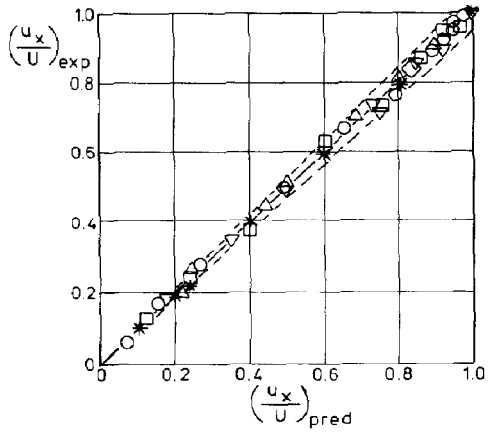

Fig. 15. Comparison of values (u_x/U) obtained experimentally and as the result of numerical simulation with values predicted from eq. (9). Experimental data points and numerical results. ○: $Re = 15.3$ ($L_v = 4.51 \times 10^{-3}$ m), □: $Re = 43.2$ ($L_v = 1.71 \times 10^{-3}$ m), ▽: $Re = 154$ ($L_v = 4.44 \times 10^{-3}$ m), △: $Re = 408$ ($L_v = 1.66 \times 10^{-3}$ m), ◇: $Re = 635$ ($L_v = 1.09 \times 10^{-3}$ m). Numerical results (———) $Re = 35{,}000$ ($L_v = 1.94 \times 10^{-6}$ m). (– – – – –) ± 5% limit.

It is now possible to quantify the concept of an approach length on the basis of a 99% criterion. This means that the approach length L_a can be defined as the upstream distance where the actual velocity differs by less than 1% from the undisturbed velocity. Introducing this condition into eq. (12) gives after recalculation:

$$\frac{|L_a|}{A} = 99 + \frac{426}{\sqrt{Re_A}}. \tag{13}$$

Apart from phenomena in the horizontal direction, also vertical velocity components and pressure gradients occur in the upstream region. These have been investigated only numerically; their magnitudes prevented an accurate experimental verification.

In Fig. 16 profiles of the dimensionless vertical velocity u_y/U as calculated for a Reynolds number of

635 are presented as a function of the dimensionless upstream distance x/L_a. From this graph it follows that the vertical components of the velocity develop in the upstream region with maximal values close to the entry plane. Despite the fact that the values of this velocity components are relatively small (with a maximum of 20% of the entrance velocity) for accurate calculations it has to be recognized that the flow in upstream region is essentially two-dimensional.

In Figs 17 and 18 the pressure distributions in horizontal and vertical direction are shown as calculated for a Reynolds number of 635. These diagrams are plotted respectively as the dependence of dimensionless pressure $p/(\frac{1}{2}\rho U^2)$ on the dimensionless upstream distance x/L_a and dimensionless vertical distance. As would be expected the highest values of the pressure can be found in the neighbourhood of the stagnation point.

The dimensionless value of the stagnation pressure p_s defined as $p_s/(\frac{1}{2}\rho U^2)$ at the leading edge is presented as a function of Reynolds number in Fig. 19. Numerical results have been extended here by data points for Reynolds numbers equal to 9, 3 and 1.5. Problems with convergence did not allow to perform simulations for lower values of the Re criterion.

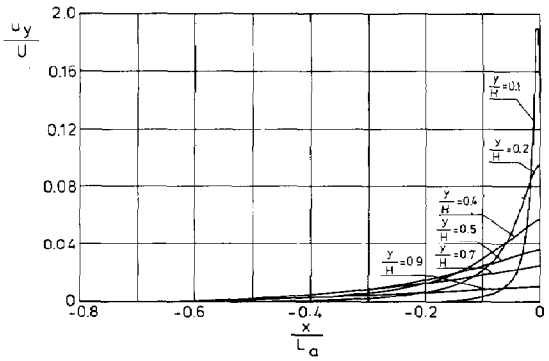

Fig. 16. The dependence of the dimensionless vertical velocity on the dimensionless upstream distance for $Re = 635$ ($L_v = 1.09 \times 10^{-3}$ m).

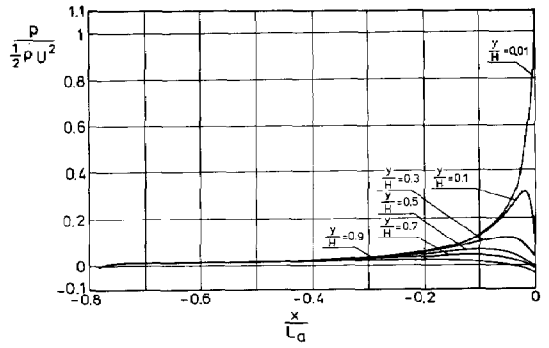

Fig. 17. The dependence of the dimensionless pressure on the dimensionless upstream distance for $Re = 635$ ($L_v = 1.09 \times 10^{-3}$ m).

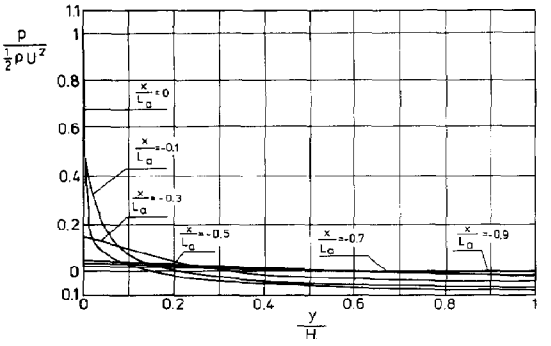

Fig. 18. The dependence of the dimensionless pressure on the dimensionless vertical distance for $Re = 635$ ($L_v = 1.09 \times 10^{-3}$ m).

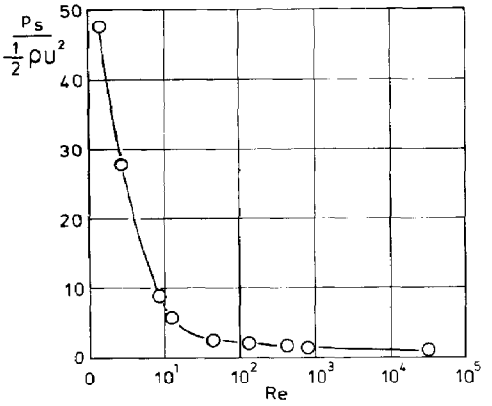

Fig. 19. Changes of the dimensionless pressure in the stagnation point as a function of Re number.

Figure 19 confirms that for large Reynolds numbers the dimensionless pressure approaches unity as can be expected from the theory of flow of a non-viscous liquid towards a stagnation point (Schlichting, 1979). This can also be viewed as a confirmation of eq. (13) which predicts a constant value of the approach length at high values of Reynolds numbers.

In case of flows at low values of Reynolds numbers the slope of the line in Fig. 19 approaches a constant value. Therefore, pressure rise in the stagnation point becomes proportional to the liquid viscosity and velocity as predicted for instance by the Stokes equation for a sphere.

6. CONCLUSIONS

From experiments as well as from numerical simulations it can be concluded that there exists a definite distortion of the velocity profile in front of the entry plane of the flow conduit. A good agreement between LDA experiments and numerical simulations could be obtained. The distortion of the flow profile in front of the entry affects the classical contention of boundary

layer built up, and as a result the boundary layer at the leading edge of a wall of a channel will have a finite thickness. As a consequence the shear stress at the tip will have finite thickness. The distortion is essential for the flow in front of the plate and contrary to common belief is not restricted to a small range of Reynolds numbers. Even for hypothetical simulations of a laminar flow extended to unrealistically (high) Reynolds numbers ($Re = 35{,}000$) the distortion remained prominent.

The flow profile in front of the edge of the plate can be modelled by an extension of the source theory for flow. Good results are obtained by a superposition of the classical source strength for inviscous flow and a contribution for the influence of the viscosity. From the source approximation an approach length can be derived, where the influence of the stagnation point is noticeable. This approach length is inversely proportional to the square root of the Reynolds number Re_A and approaches at large values of the Reynolds number a constant value.

An extra verification of the results can be obtained by the pressure distribution as derived from the velocity profiles in front of the plate. As has to be expected, the pressure at the stagnation point approaches the value for inviscous flow at high Reynolds numbers and matches creeping flow conditions at a low value of the Reynolds number.

In this work the problems of flow profile development were considered for the case of laminar flow in an open channel approaching a flat plate. It seems however that the same phenomena can be expected during the flow of fluids in other geometries, e.g. between parallel plates or at the entry of a tube flow, provided the boundary conditions are adjusted properly.

Acknowledgement– This project has been sponsored by the Foundation for Chemical Research in the Netherlands (SON) a division of the Dutch Organisation for the Advancement of Pure Research (NWO).

NOTATION

a_u	distance of a source from the edge of the wall, m
A	constant in eq. (9), m
B	constant in eq. (9), $\sqrt{\text{m}}$
Fr	Froude number
g	gravitational acceleration, m/s^2
H	height of the flow domain, m
H_t	height of the liquid in the tunnel, m
l	distance along the tunnel, m
L_a	approach length, m
L_v	viscous length, m
p	pressure, Pa
p_s	stagnation pressure, Pa
q	strength of the source, m^2/s
Re	Reynolds number
Re_A	Reynolds number defined by eq. (10)
u_x, u_y	local components of a velocity, m/s
$\mathbf{u}$	velocity vector, m/s
U	velocity of undisturbed stream, m/s
x, y, z	coordinates, m

Greek letters

$\boldsymbol{\delta}$	unit tensor
∇	Nabla operator
μ	liquid viscosity, Pa s
$\boldsymbol{\tau}$	shear stress tensor, Pa
ρ	liquid density, kg/m^3

REFERENCES

Astarita, G. and Greco, G., 1968, Excess pressure drop in laminar flow through sudden contraction. *Ind. Engng Chem. Fund.* **7**, 27–34.

Boger, D. V., 1982, Circular entry flows of inelastic and viscoelastic fluids, in *Advances in Transport Processes* (Edited by A. S. Mujumdar and R. A. Mashelkar), Vol. 2, pp. 43–98. Wiley Eastern, New Delhi.

Christiansen, E. B., Kelsey, S. J. and Carter, T. R., 1972, Laminar tube flow through an abrupt contraction. *A.I.Ch.E. J.* **18**, 372–380.

Durst, F., Melling, A. and Whitelaw, J. H., 1976, *Principles and Practice of Laser–Doppler Anemometry*. Academic Press, London.

Fluent Manual, 1987, Creare Incorporated, Hanover.

Granger, R. A., 1985, *Fluid Mechanics*, pp. 624–625. Holt–Saunders Int., New York.

Gupta, S. C. and Garg, V. K., 1981, Developing flow in a concentric annulus. **28**, 27–35.

Gupta, R. C., 1984, Power fluid flow in the hydrodynamic inlet region of a straight channel. *J. Phys. Soc. Japan* **53**, 585–591.

Mohanty, A. K. and Asthana, S. B. L., 1979, Laminar flow in the entrance region of a smooth pipe. *J. Fluid Mech.* **90**, 433–447.

Mohanty, A. K. and Das R., 1982, Laminar flow in the entrance region of a parallel plate channel. *A.I.Ch.E. J.* **28**, 831–833.

Schlichting, H., 1979, *Boundary Layer Theory*, pp. 96–98. McGraw-Hill, New York.

Soh, W. Y., 1987. Time marching solution of incompressible Navier–Stokes equations for internal flow. *Comput. Phys.* **70**, 232–252.

Sylvester, N. D. and Rosen, S. L., 1970, Laminar flow in the entrance region of a cylindrical tube. *A.I.Ch.E. J.* **16**, 964–966.

Tachibana, M. and Iemoto, Y., 1981, Steady laminar flow in the inlet region of rectangular ducts. *Bull. JSME* **24**, 1151–1158.

Van Dyke, M., 1970, Entry flow in channel. *J. Fluid Mech.* **44**, 813–823.

Vrentas, J. S., Duda, J. L. and Bargeron, K. G., 1966, Effect of axial diffusion of vorticity on flow development in circular conduits. *A.I.Ch.E. J.* **12**, 837–844.

Wang, Y. L. and Longwell P. A., 1964, Laminar flow in the inlet section of parallel plates. *A.I.Ch.E. J.* **10**, 323–329.

Zirilli, F. and Wirtz, R. A., 1983, A collocation finite element–finite difference solution for developing isothermal flow between two parallel plates. *Comput. Fluids* **11**, 379–390.